

# Unleashing Generalization of End-to-End Autonomous Driving with Controllable Long Video Generation

Enhui Ma<sup>1,2,3\*</sup> Lijun Zhou<sup>2\*</sup> Tao Tang<sup>4,2</sup> Zhan Zhang<sup>5,1</sup> Dong Han<sup>6,1</sup> Junpeng Jiang<sup>7,2</sup>  
 Kun Zhan<sup>2</sup> Peng Jia<sup>2</sup> Xianpeng Lang<sup>2</sup> Haiyang Sun<sup>2</sup> Di Lin<sup>3</sup> Kaicheng Yu<sup>1†</sup>  
<sup>1</sup>Westlake University <sup>2</sup>Li Auto Inc. <sup>3</sup>Tianjin University <sup>4</sup>Shenzhen Campus, Sun Yat-sen University  
<sup>5</sup>Southeast University <sup>6</sup>Harbin Engineering University <sup>7</sup>Harbin Institute of Technology(Shenzhen)

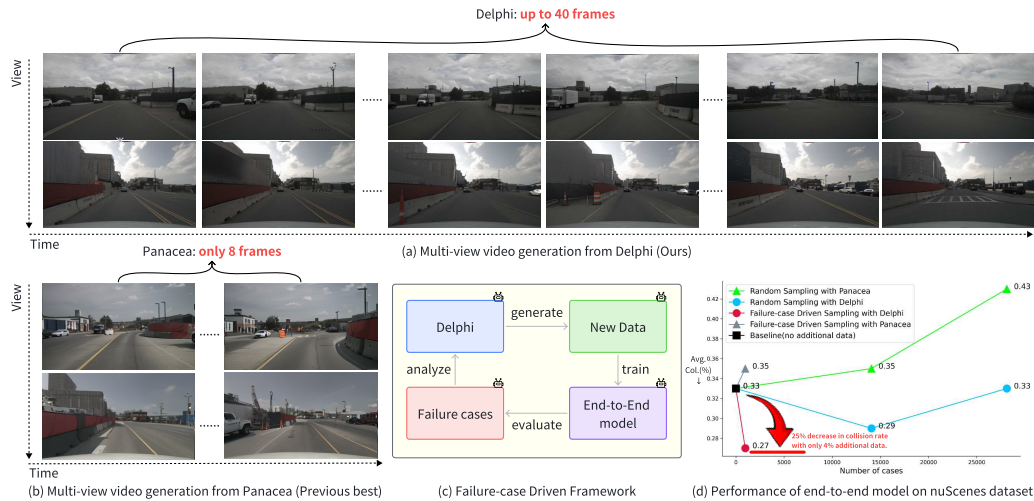


Figure 1: **Overview of our method.** We show that (a) our *Delphi* can generate up to 40 frames consecutive videos while (b) existing best only generate 8 frames. (c) With the failure-cased driven framework equipped with *Delphi*, (d) we can significantly boost the end-to-end model performance with much smaller cost.

## Abstract

Using generative models to synthesize new data has become a de-facto standard in autonomous driving to address the data scarcity issue. Though existing approaches are able to boost perception models, we discover that these approaches fail to improve the performance of planning of end-to-end autonomous driving models as the generated videos are usually less than 8 frames and the spatial and temporal inconsistencies are not negligible. To this end, we propose *Delphi*, a novel diffusion-based long video generation method with a shared noise modeling mechanism across the multi-views to increase spatial consistency, and a feature-aligned module to achieves both precise controllability and temporal consistency. Our method can generate up to 40 frames of video without loss of consistency which is about 5 times longer compared with state-of-the-art methods. Instead of randomly generating new data, we further design a sampling policy to let *Delphi* generate new data that are similar to those failure cases to improve the sample efficiency. This is achieved by building a failure-case driven framework with the help of pre-trained visual language models. Our extensive experiment demonstrates that our *Delphi* generates a higher quality of long videos surpassing previous state-of-the-art methods. Consequentially, with only generating 4% of the training dataset size, our framework is able to go beyond perception and prediction tasks, for the

\*Co-first authors

†Corresponding Author

first time to the best of our knowledge, boost the planning performance of the end-to-end autonomous driving model by a margin of 25%. Please see visual demos at <https://westlake-autolab.github.io/delphi.github.io/>.

## 1 Introduction

End-to-end autonomous driving has recently garnered increasing attention [13, 16, 43], which directly learns to plan motions from raw sensor data, reducing heavy reliance on hand-crafted rules and avoiding cascading modules. However, current end-to-end models face significant challenges in the scale and quality of training data. Insufficient data diversity can lead to model overfitting [44], such as the collected real-world trajectories mainly involve straight lines for the "go straight" action, when applied to more complex scenarios like "turn left on cross intersection", the model is prone to fail. While large-scale and high-quality annotated data is crucial for the safe and robust end-to-end autonomous driving system, unfortunately, collecting such data poses challenges, particularly in situations involving dangerous scenes where data collection can be difficult or unsafe.

Although recent generative models [5, 40, 42] have gained remarkable progress in mitigating the problem of data scarcity for perception models, which is achieved by employing ControlNet [46] to control the geometric position of scene elements with injected BEV layouts and extend across the view dimension to generate multi-view images. When applied to end-to-end autonomous driving which requires long multi-view videos, two main challenges arise: **spatial-temporal consistency** and **precise controllability**. Existing generative methods [5, 40, 38, 39] simply utilize cross-frame attention with the previously generated frame to ensure consistency, which overlooks the differences in noise patterns between image generation and video generation, as well as the alignment of features in the cross-frame attention. As a result, temporal consistency can only be maintained in short video sequences, such as Panacea [40] with 8 frames and MagicDrive [5] with 7 frames. Furthermore, current methods only offer coarse-grained control over the generated videos, limited to modifying simple global attributes, such as changing weather with simple text prompts. They cannot finely control the overall architectural style of the scene or the specific appearance attributes of individual objects.

To this end, we propose a novel multi-view long video generation method, dubbed *Delphi*, to address these limitations. First, we notice that existing approaches fall short in two aspects: i) adding independent noise to different views and does not consider the cross-view consistency; ii) exploiting a simple cross attention to fuse multiple feature spaces with different reception fields. We then propose two components, a noise reinitialization module to model the shared noise across frames and a feature-aligned temporal consistent module to address the second challenge.

Leveraging *Delphi* as the data engine, we further propose a failure-case driven framework, which automatically enhances the generalization of end-to-end models. Specifically, this framework integrates several steps as shown in Figure 1: 1) evaluating the end-to-end model, collecting failure cases, 2) analyzing the implicit data patterns using pre-trained VLMs, 3) retrieving similar patterned data from existing training data, 4) generating diverse training data with *Delphi*, and then updating the end-to-end model. To investigate the effectiveness of our method, we conducted extensive experiments on the large-scale public dataset nuScenes [2]. Firstly, comprehensive evaluations with various metrics demonstrate that our *Delphi* generate high-quality long multi-view videos with spatiotemporal consistency and precise controllability. Furthermore, the proposed failure-case driven framework achieves remarkable improvement in the generalization capability of end-to-end models at a low cost.

Our contributions can be summarized as follows:

- We introduce *Delphi*, a novel method that can generate up to 12 seconds (40 frames) temporally consistent multi-view videos in autonomous driving (AD) scenarios, which is 5x longer compared to the state-of-the-art video generation methods. In addition, *Delphi* encompasses the control ability including both object and scene level details to enrich the diversity of generated data.
- We propose a failure-case driven framework to drastically increase sampling efficiency. We show that using a long-term video generation method that trained purely on the training dataset, we are able to improve the UniAD’s performance by 25% (collision rate reduces from 0.34 to 0.27) from with generating only 4% (972 cases) of the training dataset size.

- Compared to earlier works that only manage to improve the perception ability using synthetic data, we are the first, to the best of our knowledge, to showcase that a data engine can go beyond the perception task and automatically improve the planning ability of end-to-end AD methods. We hope this can shed light on alleviating the long-tail issue of the large-scale development of AD vehicles.

## 2 Related work

**End-to-end Autonomous Driving.** End-to-end models have garnered significant attention in the field of autonomous driving. These models simplify the traditional modular pipeline by integrating perception, prediction, decision, and planning into a single learning framework. TransFuser[25] fuses visual and lidar inputs with a transformer-based architecture to improve perception and driving decisions. ST-P3[12] leverages spatial-temporal feature learning to improve perception, prediction, and planning tasks. UniAD[13] effectively combines multiple perception and prediction tasks to improve planning performance. VAD [16] explores the potential of vectorized scene representation for planning and getting rid of dense maps. VADv2[3] utilizes probabilistic planning to manage uncertainties and transforms multi-view image sequences into environmental token embeddings to predict and sample vehicle control actions. In this paper, we have opted to utilize the well-known UniAD as our downstream model due to the computational resource constraints.

**Generative model to boost autonomous driving performance.** Video generation stands as a pivotal technology in understanding the visual world. Early methods mainly include Variational Autoencoders (VAEs) [4, 14], flow-based models [18], and Generative Adversarial Networks (GANs) [23, 30, 34, 36]. Notably, the recent achievements of diffusion models in image generation [24, 28, 29] have stimulated interest in their application to video generation [6, 10]. Diffusion-based methods have significantly improved realism, controllability, and temporal consistency. With their controllable attributes, text-based conditional video generation has garnered increasing attention, leading to the emergence of numerous methods [28, 9, 31, 41, 48]. Especially popular models like diffusion-based models [28, 32, 8, 46], which enable users to generate images with controllability. Inspired by this innovation, some models [5, 42] employ ControlNet to control the geometric position of scene elements by injecting BEV layouts and extend this approach across the view dimension to generate multi-view images. The other models [40, 38, 47] further extend this to the temporal dimension to generate multi-view videos, which are all trained based on the pre-trained image models [28]. BEVGen [33] specializes in generating multi-view street images based on Bird’s Eye View (BEV) layouts. BEVControl [42] proposes a two-stage generation pipeline for creating image foregrounds and backgrounds from BEV layouts. DriveDreamer [38] and Panacea [40] introduce a layout-conditioned video generation system aimed at diversifying data sources for training perception models. GAIA-1 [11] and ADriver-I [15] integrate large language models into video generation; a concurrent work DriveDreamer-2 [47] proposes a traffic simulation pipeline employing only text prompts as input, which can be utilized to generate diverse traffic conditions for driving video generation, however, it requires one frame input and does not work in the setting of boosting planning task. All in all, these methods can only generate fairly short videos up to 8 frames, while our *Delphi* can generate much longer ones.

## 3 Method

In this section, we first present *Delphi*, an innovative method for generating long multi-view videos of autonomous driving. There are two core modules designed for generating temporally consistent videos: Noise Reinitialization Module (NRM) in Sec 3.1.1 and Feature-aligned Temporal Consistency Module (FTCM) in Sec 3.1.2. Finally, Sec. 3.2 presents a failure-case driven framework to show how we can leverage the long-term video generation ability to automatically enhance the generalization of an end-to-end model with only data from the training dataset.

### 3.1 Delphi: A Controllable Long Video Generation Method

Here, we present the architecture of *Delphi* in Figure 2(a). Existing models tend to overlook the noise formulation across time and spatial dimensions, leading to inferior long-video generation quality. In

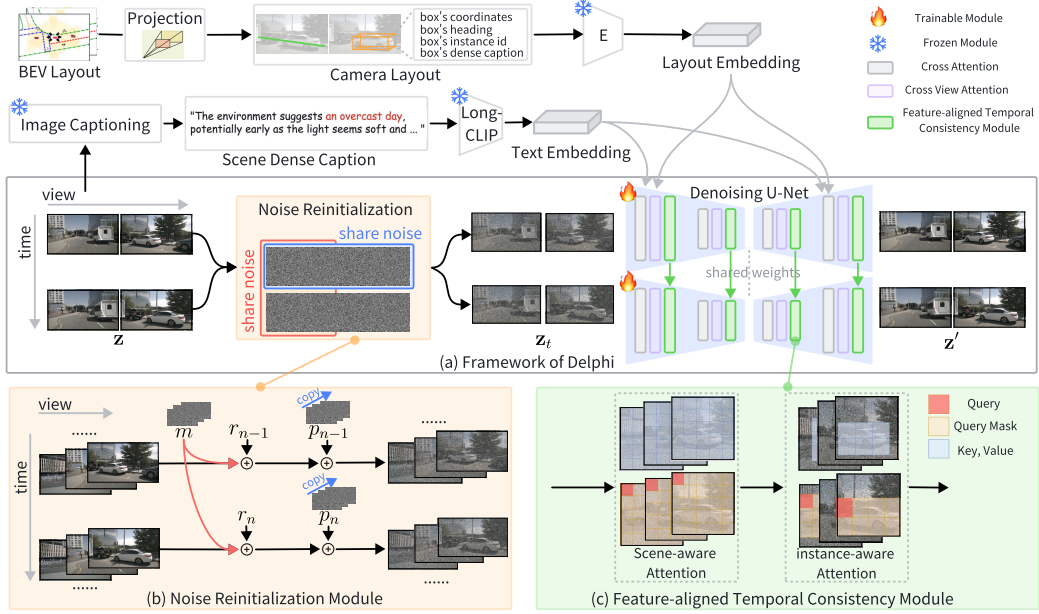


Figure 2: **(a) Architecture of Delphi.** It takes multi-view videos  $\mathbf{z}$  and the corresponding BEV (Bird’s Eye View) layout sequences as input. Each video consists of  $N$  frames and  $V$  views. The BEV layout sequences are first projected into camera space according to camera parameters, resulting in camera layouts that include both foreground and background layouts. Specifically, the foreground layout includes the bounding box’s corner coordinates, heading, instance id, and dense caption, while the background one includes different colored lines to represent road trends. The layout embeddings, processed by the encoder, are injected into the U-Net through cross-attention to achieve fine-grained layout control in the generation process. Additionally, we leverage VLM [1] to extract dense captions for the input scenes, which are encoded by Long-CLIP [45] to obtain text embeddings, which are then injected into the U-Net via text cross-attention to achieve text-based control. We further design two key modules, **(b) Noise Reinitialization Module** that encompass a share noise across different views and **(c) Feature-aligned Temporal Consistency Module** to ensure spatial and temporal consistency accordingly.

contrast, we propose two key components to address these challenges: a noise reinitialization module and a feature-aligned temporal consistency module.

### 3.1.1 Noise Reinitialization Module

Multi-view videos naturally exhibit similarities across both time and view dimensions. However, existing approaches are categorized into two groups, i) concurrent single-view video generation methods [22, 27, 26] cannot be directly applied in outdoor multi-view scenarios; ii) multi-view generative models are adding independent noise that does not consider cross view consistencies [5, 42, 40]. Here, we plan to address this issue by introducing a shared noise across these two dimensions. Specifically, as shown in Figure 2(b), we introduce shared motion noise  $m$  along the temporal dimension and shared panoramic noise  $p$  along the viewpoint dimension. This results in a noisy version of the multi-view video that is correlated across both time and view dimensions. The process of incorporating shared noise can be represented as follows:

$$\mathbf{z}_n^v = \sqrt{\hat{\alpha}}x_n^v + \sqrt{1 - \hat{\alpha}}(r_n^v + m^v + p_n), \quad (1)$$

where  $\mathbf{z}_n^v \in \mathbb{R}^{1 \times 1 \times h \times w}$  represents the image latent variable of view  $v$  at frame  $n$ ,  $m \in \mathbb{R}^{V \times 1 \times h \times w}$  are the shared motion noise of  $V$  views, and  $p \in \mathbb{R}^{1 \times N \times h \times w}$  are the shared panoramic noise of  $N$  frames. For simplicity, we omit the subscript  $t$ .

### 3.1.2 Feature-aligned Temporal Consistency

Existing methods [40, 5, 39], when generating the current frame, exploits a simple cross-attention mechanism to fuse previous frame information into the current view. However, they tend to overlook the fact that features located at different network depths possess varying receptive fields. Consequently, this coarse feature interaction method fails to capture all the information from the receptive fields from different levels of the previous frame, leading to sub-optimal video generation performance.

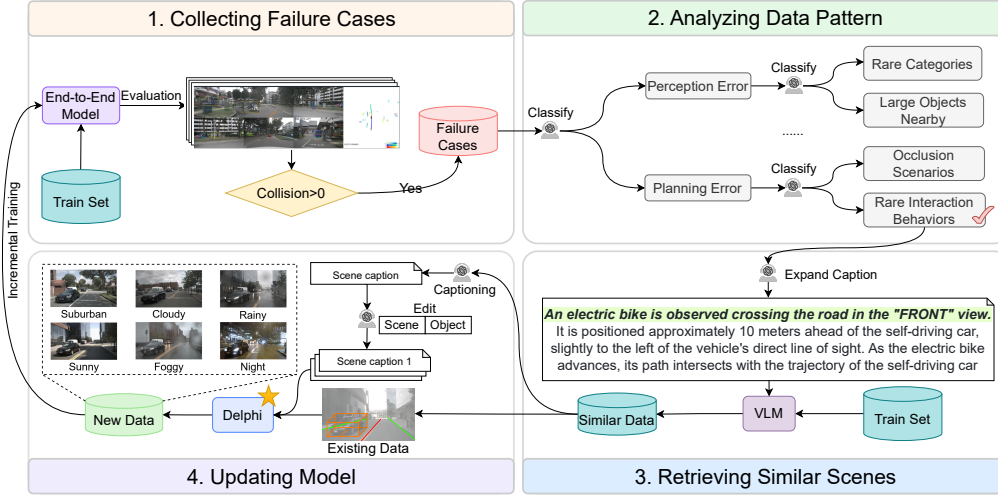


Figure 3: Overview of Failure-case Driven Framework.

To this end, we propose a more effective structure to fully establish feature interactions between aligned features at the same network depth in adjacent frames as shown in Figure 2 (c). We approach this by ensuring global consistency and optimizing local consistency, incorporating two main designs: Scene-aware Attention and Instance-aware Attention.

**Scene-aware Attention.** To fully leverage the rich information from features at different network depths in the previous frame, we propose a scene-level cross-frame attention mechanism. Specifically, this module performs the attention calculation on features at the same network depth between adjacent frames. The computation process can be represented as follows:

$$\text{Attn}_{\text{scene}}(Q_n^i, K_{n-1}^i, V_{n-1}^i) = \text{softmax} \left( \frac{Q_n^i K_{n-1}^i T}{\sqrt{d_k}} \right) V_{n-1}^i, \quad (2)$$

where  $Q_n^i$  (query) is the latent feature map from the current frame  $n$  at a specific network depth  $i$ ,  $K_{n-1}^i$  (key) and  $V_{n-1}^i$  (value) are the latent feature maps from the previous frame  $n - 1$  at the same network depth  $i$ , and  $d_k$  is the dimensionality of the key. And  $i = 1, \dots, I$ , where  $I$  indicates the total number of U-Net blocks. We omit the view channel for simplicity. By applying this scene-aware attention mechanism, the module effectively transfers the global style information from the previous frame to the current frame, ensuring temporal consistency across frames.

**Instance-aware Attention.** To enhance the coherence of moving objects within the scene, we propose an Instance-aware Cross-frame Attention mechanism. Compared to scene-level attention, this module uses foreground bounding boxes as attention masks to compute feature interactions in local regions between adjacent frames. The computation process can be represented as follows:

$$\text{Attn}_{\text{ins}}(Q_n^i, K_{n-1}^i, V_{n-1}^i) = \text{softmax} \left( \frac{(Q_n^i \cdot M_n)(K_{n-1}^i \cdot M_{n-1})^T}{\sqrt{d_k}} \right) (V_{n-1}^i \cdot M_{n-1}), \quad (3)$$

$$\hat{Q}_n^i = Q_n^i + \text{Zero}[\text{Attn}_{\text{ins}}(Q_n^i, K_{n-1}^i, V_{n-1}^i)]q, \quad (4)$$

where  $M_n$  and  $M_{n-1}$  are the masks of foreground objects from the current frame and previous frame respectively, focusing on the region defined by the foreground bounding box, and Zero indicates the trainable convolution layers initialized with a value of 0.

### 3.2 Failure-case Driven Framework

In order to leverage the generated data, common approaches will randomly sample a subset of the training dataset and then apply video generation models to augment these data to enhance the performance of downstream tasks. We hypothesize that this random sample does not consider the

Table 1: We compare Delphi with state-of-the-art methods on the nuScenes validation set. The results measure the spatial-temporal consistency and controllability of different methods.  $\downarrow/\uparrow$  means a smaller/larger value of the metric represents a better performance.

| Method            | Spatial Consistency |                 | Temporal Consistency |              |              | Sim-Real Gap   |                             |
|-------------------|---------------------|-----------------|----------------------|--------------|--------------|----------------|-----------------------------|
|                   | FID $\downarrow$    | CLIP $\uparrow$ | FVD $\downarrow$     |              |              | NDS $\uparrow$ | Avg. Col. Rate $\downarrow$ |
|                   |                     |                 | 4 frames             | 8 frames     | 40 frames    |                |                             |
| BEVGen [33]       | 25.54               | 71.23           | N/A                  | N/A          | Fail         | N/A            | N/A                         |
| BEVControl [42]   | 24.85               | 82.70           | N/A                  | N/A          | Fail         | N/A            | N/A                         |
| DriveDreamer [38] | 26.8                | N/A             | N/A                  | 353.2        | Fail         | N/A            | N/A                         |
| MagicDrive [5]    | 16.20               | N/A             | N/A                  | N/A          | Fail         | N/A            | N/A                         |
| MagicDrive* [5]   | 46.18               | 82.47           | 617.2                | N/A          | Fail         | 34.56          | 3.87                        |
| Panacea [40]      | 16.96               | N/A             | N/A                  | 139.0        | Fail         | 32.10          | N/A                         |
| Panacea* [40]     | 55.32               | 84.23           | –                    | 446.9        | Fail         | 29.41          | 1.35                        |
| Drive-WM [39]     | 15.8                | N/A             | N/A                  | 122.7        | Fail         | N/A            | N/A                         |
| Delphi (Ours)     | <b>15.08</b>        | <b>86.73</b>    | –                    | <b>113.5</b> | <b>275.6</b> | <b>36.58</b>   | <b>0.29</b>                 |

\* Results are computed using the official github release code or rendered videos on validation set.

N/A indicates the model or the pre-trained weights is not open-sourced so we cannot faithfully reproduce.

existing distribution of long-tail cases and is substantial for further optimization. We hence propose a simple but effective failure-case driven framework that exploits four steps to reduce the computational costs. As shown in Figure 3, we first evaluate the existing failure cases as a starting point, we then implement a visual language-based method to analyze the patterns of these data and retrieve similar scenes to gain a deeper understanding of the context, we then diversify the captions for scene and instance editing, to generate new data with different appearances. Finally, we train the downstream tasks with such additional data for a few epochs to increase the generalization ability.

Note that, all of these operations are conducted on training set to avoid any potential leak of the validation information. Please see supplementary materials for detailed implementation of each component. In addition, we notice a concurrent work [20] that exploits a similar idea. However, their approach only works for 2D detection tasks while our method is capable of improving end-to-end planning ability.

## 4 Experiments

We follow popular methods [40, 42], to use nuScenes [2] and use FID [7], FVD [35], and downstream model’s performances on newly generated data to evaluate the image, video, and sim-to-real gap. See the Appendix for more details.

**Dataset.** We conduct extensive experiments on the popular nuScenes [2] validation dataset, which comprises 150 driving scenes marked by dense traffic and intricate street driving scenarios. Each scene contains roughly 40 frames. We utilize ten foreground categories (i.e., bus, car, bicycle, truck, trailer, motorcycle) to create detailed street foreground object layouts. Four background classes obtained from the map expansion pack are used to generate background layouts.

**Hyperparameters.** We train our models on 8 A800 80GB GPUs. The diffusion U-Net is optimized using the AdamW [17] optimizer with a learning rate of  $5e-5$ . We resize the original images from  $1600 \times 900$  to  $512 \times 512$ . During training, the video length is set to 10, and we generate video frames sequentially in a streaming manner. For inference, we use the PLMS [21] sampler configured with 50 sampling steps. The spatial resolution of the video samples is set to  $512 \times 512$ , with a frame length of 40. The inference length is not restricted and could be 40 or longer. Our model is trained on the nuScenes dataset with 50,000 steps for the cross-view model and 20,000 steps for the temporal model.

### 4.1 Comparing Delphi to state-of-the-art video generation methods

We assess the quality of video generation through a comprehensive evaluation encompassing both quantitative and qualitative aspects, comparing our approach with previous methodologies. In Table 1, we report the metrics in three aspects on nuScenes validation set, spatial and temporal consistency, and sim-real gap. In short, our method surpasses the state-of-the-art by a clear margin, on short video generation tasks, and can generate videos up to 40 frames. In contrast, the other methods collapse, which proves the effectiveness of our method in long-term video generation. We show qualitative

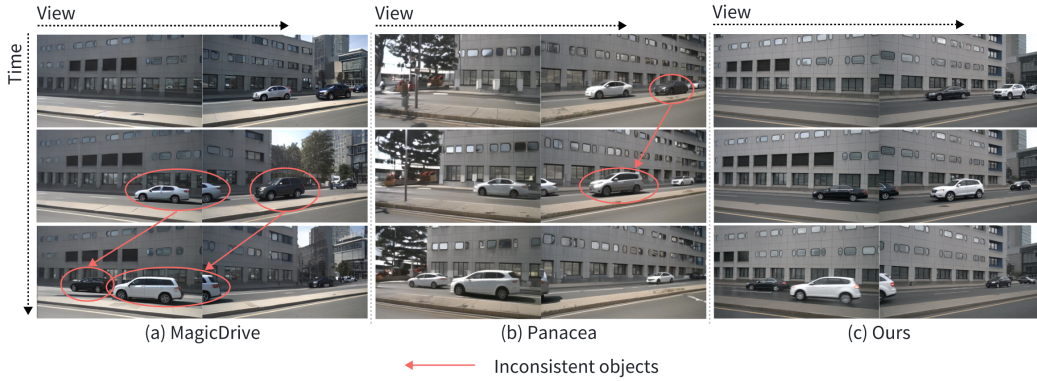


Figure 4: **Visual comparison of local region generated by different generative models.**

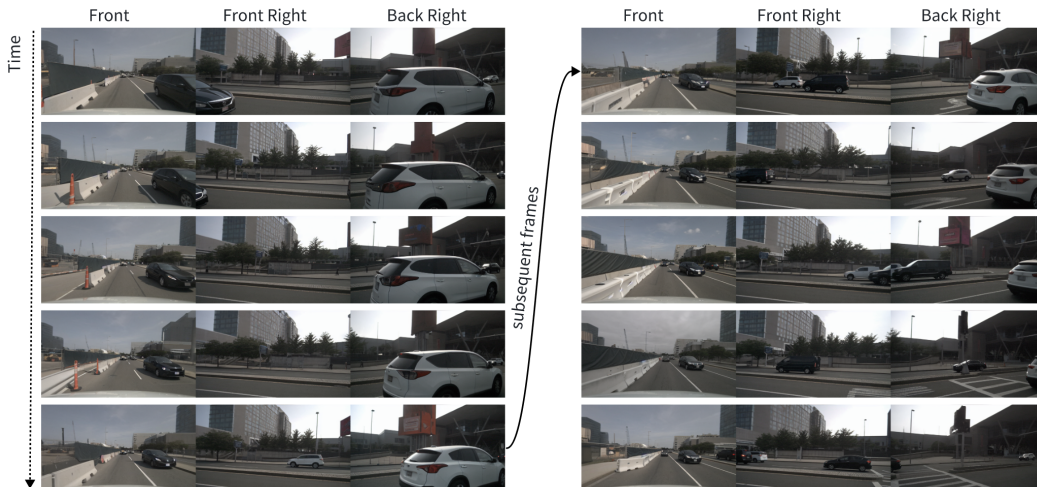


Figure 5: **The multi-view long video with spatiotemporal consistency generated by Delphi.**

results in Figure 4 and compare the video quality with previous methods on the same clip. Our method maintains consistent spatial and temporal appearance where the previous methods fail.

**Visualization of multi-view long videos generated by Delphi.** We demonstrate the generated multi-view long video in Figure 5. It can be seen that our method has the powerful ability to generate long videos with spatiotemporal consistency.

**Visualization comparison of multi-view video generated by different models.** We demonstrate visualization comparisons of multi-view video generated by different models in Figure 6. It can be seen that our method has the powerful ability to generate long videos with spatiotemporal consistency.

**4.2 Our failure-case driven framework boosts the end-to-end planning model**

To prove the effectiveness of our framework, we compare three factors in Table 2, the number of generated cases, data engine (video generation method), and the choice of data source. In summary, we discover that, by generating only 4% of the training set size data, our method can reduce the collision rate from 0.33 to 0.27 by a margin of 25%. However, under the same setting, the collision rate increases if we use other data engines such as Panacea to fine-tune the UniAD. Nonetheless, we also exploit random sampling for both data engines and our method constantly outperforms the baseline. We also show how our frameworks can fix failure cases in Figure 7.

**What if we sample the layouts from the validation set?** Since our Delphi only sees the training set of nuScenes, a natural question is, can we include the validation set to see if we can further boost the performances of downstream tasks? Here, we collect failure cases from both the training and validation sets. Note that, since only layouts and captions are used in our framework, *the validation video clips are never exposed in any training processes.* We notice that the collision rate is reduced from 0.33 to 0.26 with merely generating 429 cases, which is only 1.5% of the training set size. This



Figure 6: Visualization comparison of multi-view video generated by different models.

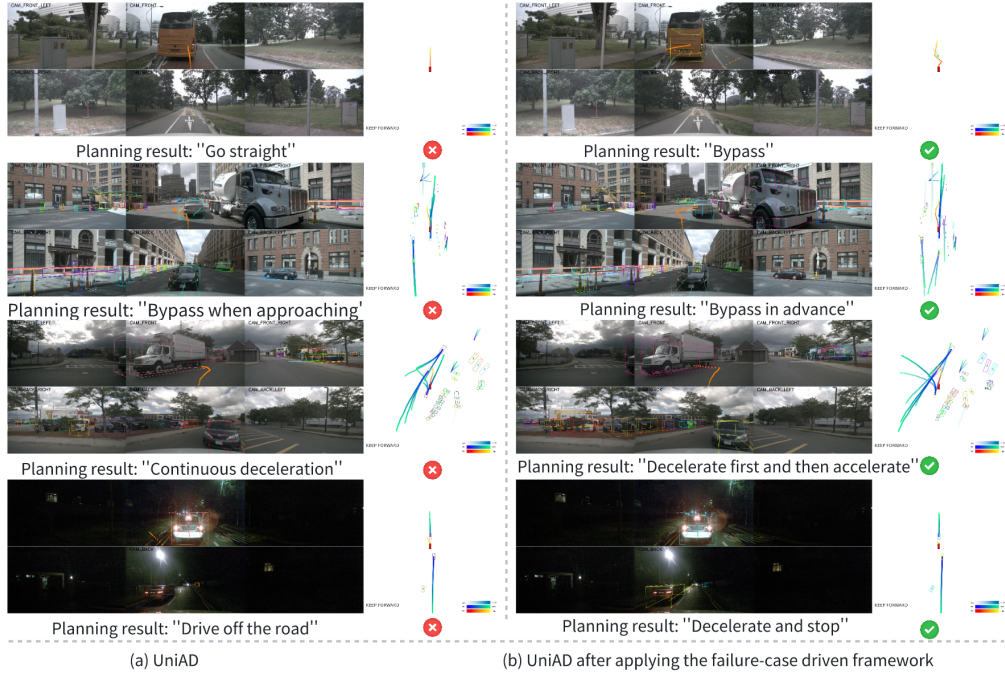


Figure 7: Visualization of four examples before and after. (a) Here, we show four hard examples from the validation set, “large objects in the front” and “unprotected left turn at intersection”. (b) Our framework is able to fix these four examples without using these data during training.

Table 2: Performance comparison of the end-to-end models fine-tuned from the UniAD open source model by applying different data sampling strategies, numbers of data cases, data engines, and data sources in the failure-case driven framework. The baseline performance is presented in the first row of the table.

| Sampling Strategy            | Num of Cases | Data Engine | Data Source    | Col. Rate(%)↓ |             |             | Avg.        |
|------------------------------|--------------|-------------|----------------|---------------|-------------|-------------|-------------|
|                              |              |             |                | 1s            | 2s          | 3s          |             |
| Baseline(UniAD)              | —            | —           | —              | 0.10          | 0.18        | 0.71        | 0.33        |
| Random Sampling              | 14065 (50%)  | Panacea     | Training Set   | <b>0.03</b>   | 0.23        | 0.79        | 0.35        |
|                              |              | Delphi      |                | 0.08          | 0.20        | 0.58        | 0.29        |
|                              | 28130 (100%) | Panacea     |                | 0.08          | 0.22        | 0.98        | 0.43        |
| Delphi                       |              | 0.07        | 0.29           | 0.65          | 0.33        |             |             |
| Failure-case Driven Sampling | 972 (4%)     | Panacea     | Training Set   | 0.05          | 0.18        | 0.81        | 0.35        |
|                              |              | Delphi      |                | 0.08          | 0.18        | <b>0.56</b> | <b>0.27</b> |
|                              | 429 (1.5%)   | Delphi      | Validation Set | 0.07          | <b>0.10</b> | 0.61        | <b>0.26</b> |

result might be interesting to industrial practitioners that a diffusion-based approach that only sees training dataset videos can effectively boost the performance of the validation set with layout and captions.



Figure 8: **Visualization of instance and scene editing.** (a) shows the instance-level control result, such as the appearance attributes of all vehicles. (b) shows the scene-level control result, including weather and time.

### 4.3 Ablation Studies

We perform ablation studies to showcase the effectiveness of our method.

**Ablating Sim-Real Gap.** To further evaluate the sim-to-real gap, we train the UniAD with different portions of synthetic data. At the top of Table 3, we train UniAD with purely generated video clips, and the collision rate increases from 0.34 to 0.50. This indicates that the synthetic data cannot yet fully replace the real data. By contrast, if we consider the incremental learning setting, while we train UniAD with additional data, using synthetic data results in a much better performance while using additional real data deteriorates the performance from 0.34 to 0.38.

**Ablating Scene and Instance Editing.** Table 4 demonstrates the effectiveness of data diversity for end-to-end models. Specifically, we edited existing scenes in two approaches: scene-level editing and instance-level editing. This fancy function allows us to generate a large amount of new data from a limited amount of existing data. As shown in Table 4, simultaneous editing of both the scene and instances yields the best performance. Leveraging powerful precise controllability, Delphi maximizes end-to-end model performance by generating richer and more diverse data.

**Ablating NRM and FTCM.** In Table 5, we validate the two modules, the Noise Reinitialization Module (NRM) and the Feature-aligned Temporal Consistency Module (FTCM). We see an evident increase in all metrics to validate the effectiveness of our proposed method. In particular, the FTCM structure improves FID from 22.85 to 19.81 while the NRM further boosts it.

## 5 Conclusion

In summary, we propose a novel video generation method for autonomous driving scenarios that can synthesize up to 40 frames of videos on nuScenes dataset. Surprisingly, we show that with a diffusion model trained only with training split, we are able to improve the performance of the end-to-end planning model by a sample efficient failure-case driven framework. We hope to shed light on addressing the data scarcity problem for both researchers and practitioners in this field, and make a solid step towards making autonomous driving vehicles safe on the road.

Table 3: Performance of end-to-end model with real and generated data. We train the second stage of UniAD [13] with the officially released weights of the first stage as a starting point.

| Method         | Col. Rate(%)↓ |             |             |             |
|----------------|---------------|-------------|-------------|-------------|
|                | 1s            | 2s          | 3s          | Avg.        |
| Real           | 0.07          | 0.24        | 0.70        | 0.34        |
| Generated      | 0.17          | 0.37        | 0.97        | 0.50        |
| Real+Real      | <b>0.03</b>   | 0.33        | 0.77        | 0.38        |
| Real+Generated | 0.08          | <b>0.18</b> | <b>0.56</b> | <b>0.27</b> |

Table 4: The effectiveness of Delphi’s precise controllability on end-to-end models.

| Scene editing | Instance editing | Col. Rate(%)↓ |             |             |             |
|---------------|------------------|---------------|-------------|-------------|-------------|
|               |                  | 1s            | 2s          | 3s          | Avg.        |
|               |                  | 0.10          | 0.20        | 0.71        | 0.34        |
| ✓             |                  | 0.11          | 0.18        | 0.64        | 0.31        |
|               | ✓                | 0.05          | 0.20        | 0.62        | 0.29        |
| ✓             | ✓                | <b>0.08</b>   | <b>0.18</b> | <b>0.56</b> | <b>0.27</b> |

Table 5: Ablation study results for our proposed NRM and FTCM.

| Method         | FID ↓        | FVD ↓        | CLIP ↑       |
|----------------|--------------|--------------|--------------|
| Delphi         | <b>15.08</b> | <b>275.6</b> | <b>86.73</b> |
| w/o NRM        | 19.81        | 291.5        | 85.22        |
| w/o NRM & FTCM | 22.85        | 346.96       | 82.91        |

**Limitation and Societal Impact.** Our *Delphi* takes BEV layout as input to ensure the control ability, i.e. we are only capable of enriching the appearances and cannot change the layout during the synthesis processes. This leads to a limitation that our framework can be only used in an open-loop setting[2] but not the close-loop one. Yet, another limitation is when the end-to-end model performs perfectly in the training dataset, our failure-case driven sampling does not work. In terms of societal impact, we believe our method can be used to boost the performance of end-to-end models and may help the deployment of large-scale autonomous driving vehicles in the future.

## References

- [1] Josh Achiam, Steven Adler, Sandhini Agarwal, Lama Ahmad, Ilge Akkaya, Florencia Leoni Aleman, Diogo Almeida, Janko Altenschmidt, Sam Altman, Shyamal Anadkat, et al. Gpt-4 technical report. *arXiv preprint arXiv:2303.08774*, 2023.
- [2] Holger Caesar, Varun Bankiti, Alex H Lang, Sourabh Vora, Venice Erin Liong, Qiang Xu, Anush Krishnan, Yu Pan, Giancarlo Baldan, and Oscar Beijbom. nuscenes: A multimodal dataset for autonomous driving. In *Proceedings of the IEEE/CVF conference on computer vision and pattern recognition*, pages 11621–11631, 2020.
- [3] Shaoyu Chen, Bo Jiang, Hao Gao, Bencheng Liao, Qing Xu, Qian Zhang, Chang Huang, Wenyu Liu, and Xinggong Wang. Vadv2: End-to-end vectorized autonomous driving via probabilistic planning. *arXiv preprint arXiv:2402.13243*, 2024.
- [4] Emily Denton and Rob Fergus. Stochastic video generation with a learned prior. In *International conference on machine learning*, pages 1174–1183. PMLR, 2018.
- [5] Ruiyuan Gao, Kai Chen, Enze Xie, Lanqing Hong, Zhenguo Li, Dit-Yan Yeung, and Qiang Xu. Magicdrive: Street view generation with diverse 3d geometry control. *arXiv preprint arXiv:2310.02601*, 2023.
- [6] William Harvey, Saeid Naderiparizi, Vaden Masrani, Christian Weilbach, and Frank Wood. Flexible diffusion modeling of long videos. *Advances in Neural Information Processing Systems*, 35:27953–27965, 2022.
- [7] Martin Heusel, Hubert Ramsauer, Thomas Unterthiner, Bernhard Nessler, and Sepp Hochreiter. Gans trained by a two time-scale update rule converge to a local nash equilibrium. *Advances in neural information processing systems*, 30, 2017.
- [8] Jonathan Ho, Ajay Jain, and Pieter Abbeel. Denoising diffusion probabilistic models. *Advances in neural information processing systems*, 33:6840–6851, 2020.
- [9] Jonathan Ho, William Chan, Chitwan Saharia, Jay Whang, Ruiqi Gao, Alexey Gritsenko, Diederik P Kingma, Ben Poole, Mohammad Norouzi, David J Fleet, et al. Imagen video: High definition video generation with diffusion models. *arXiv preprint arXiv:2210.02303*, 2022.
- [10] Tobias Höppe. Diffusion models for video prediction and infilling: Training a conditional video diffusion model for arbitrary video completion tasks, 2022.
- [11] Anthony Hu, Lloyd Russell, Hudson Yeo, Zak Murez, George Fedoseev, Alex Kendall, Jamie Shotton, and Gianluca Corrado. Gaia-1: A generative world model for autonomous driving. *arXiv preprint arXiv:2309.17080*, 2023.
- [12] Shengchao Hu, Li Chen, Penghao Wu, Hongyang Li, Junchi Yan, and Dacheng Tao. St-p3: End-to-end vision-based autonomous driving via spatial-temporal feature learning. In *European Conference on Computer Vision (ECCV)*, 2022.
- [13] Yihan Hu, Jiazhi Yang, Li Chen, Keyu Li, Chonghao Sima, Xizhou Zhu, Siqi Chai, Senyao Du, Tianwei Lin, Wenhai Wang, et al. Planning-oriented autonomous driving. In *Proceedings of the IEEE/CVF Conference on Computer Vision and Pattern Recognition*, pages 17853–17862, 2023.
- [14] Aapo Hyvärinen and Peter Dayan. Estimation of non-normalized statistical models by score matching. *Journal of Machine Learning Research*, 6(4), 2005.

- [15] Fan Jia, Weixin Mao, Yingfei Liu, Yucheng Zhao, Yuqing Wen, Chi Zhang, Xiangyu Zhang, and Tiancai Wang. Adriver-i: A general world model for autonomous driving. *arXiv preprint arXiv:2311.13549*, 2023.
- [16] Bo Jiang, Shaoyu Chen, Qing Xu, Bencheng Liao, Jiajie Chen, Helong Zhou, Qian Zhang, Wenyu Liu, Chang Huang, and Xinggang Wang. Vad: Vectorized scene representation for efficient autonomous driving. *2023 IEEE/CVF International Conference on Computer Vision (ICCV)*, pages 8306–8316, 2023.
- [17] Diederik P Kingma and Jimmy Ba. Adam: A method for stochastic optimization. *arXiv preprint arXiv:1412.6980*, 2014.
- [18] Manoj Kumar, Mohammad Babaeizadeh, Dumitru Erhan, Chelsea Finn, Sergey Levine, Laurent Dinh, and Durk Kingma. Videoflow: A flow-based generative model for video. *arXiv preprint arXiv:1903.01434*, 2(5):3, 2019.
- [19] Junnan Li, Dongxu Li, Silvio Savarese, and Steven Hoi. Blip-2: Bootstrapping language-image pre-training with frozen image encoders and large language models. *arXiv preprint arXiv:2301.12597*, 2023.
- [20] Mingfu Liang, Jong-Chyi Su, Samuel Schuster, Sparsh Garg, Shiyu Zhao, Ying Wu, and Manmohan Chandraker. Aide: An automatic data engine for object detection in autonomous driving. *arXiv preprint arXiv:2403.17373*, 2024.
- [21] Luping Liu, Yi Ren, Zhijie Lin, and Zhou Zhao. Pseudo numerical methods for diffusion models on manifolds. *arXiv preprint arXiv:2202.09778*, 2022.
- [22] Zhengxiong Luo, Dayou Chen, Yingya Zhang, Yan Huang, Liang Wang, Yujun Shen, Deli Zhao, Jingren Zhou, and Tieniu Tan. Videofusion: Decomposed diffusion models for high-quality video generation. In *Proceedings of the IEEE/CVF Conference on Computer Vision and Pattern Recognition*, pages 10209–10218, 2023.
- [23] Michael Mathieu, Camille Couprie, and Yann LeCun. Deep multi-scale video prediction beyond mean square error. *arXiv preprint arXiv:1511.05440*, 2015.
- [24] Alex Nichol, Prafulla Dhariwal, Aditya Ramesh, Pranav Shyam, Pamela Mishkin, Bob McGrew, Ilya Sutskever, and Mark Chen. Glide: Towards photorealistic image generation and editing with text-guided diffusion models. *arXiv preprint arXiv:2112.10741*, 2021.
- [25] Aditya Prakash, Kashyap Chitta, and Andreas Geiger. Multimodal fusion transformer for end-to-end autonomous driving. In *Proceedings of the IEEE/CVF Conference on Computer Vision and Pattern Recognition (CVPR)*, 2021.
- [26] Haonan Qiu, Menghan Xia, Yong Zhang, Yingqing He, Xintao Wang, Ying Shan, and Ziwei Liu. Freenoise: Tuning-free longer video diffusion via noise rescheduling. *arXiv preprint arXiv:2310.15169*, 2023.
- [27] Weiming Ren, Harry Yang, Ge Zhang, Cong Wei, Xinrun Du, Stephen Huang, and Wenhui Chen. Consisti2v: Enhancing visual consistency for image-to-video generation. *arXiv preprint arXiv:2402.04324*, 2024.
- [28] Robin Rombach, Andreas Blattmann, Dominik Lorenz, Patrick Esser, and Björn Ommer. High-resolution image synthesis with latent diffusion models. In *Proceedings of the IEEE/CVF conference on computer vision and pattern recognition*, pages 10684–10695, 2022.
- [29] Nataniel Ruiz, Yuanzhen Li, Varun Jampani, Yael Pritch, Michael Rubinstein, and Kfir Aberman. Dreambooth: Fine tuning text-to-image diffusion models for subject-driven generation. In *Proceedings of the IEEE/CVF Conference on Computer Vision and Pattern Recognition*, pages 22500–22510, 2023.
- [30] Masaki Saito, Eiichi Matsumoto, and Shunta Saito. Temporal generative adversarial nets with singular value clipping. In *Proceedings of the IEEE international conference on computer vision*, pages 2830–2839, 2017.

- [31] Uriel Singer, Adam Polyak, Thomas Hayes, Xi Yin, Jie An, Songyang Zhang, Qiyuan Hu, Harry Yang, Oron Ashual, Oran Gafni, et al. Make-a-video: Text-to-video generation without text-video data. *arXiv preprint arXiv:2209.14792*, 2022.
- [32] Jiaming Song, Chenlin Meng, and Stefano Ermon. Denoising diffusion implicit models. *arXiv preprint arXiv:2010.02502*, 2020.
- [33] Alexander Szwedlow, Runsheng Xu, and Bolei Zhou. Street-view image generation from a bird’s-eye view layout. *arXiv preprint arXiv:2301.04634*, 2023.
- [34] Sergey Tulyakov, Ming-Yu Liu, Xiaodong Yang, and Jan Kautz. Mocogan: Decomposing motion and content for video generation. In *Proceedings of the IEEE conference on computer vision and pattern recognition*, pages 1526–1535, 2018.
- [35] Thomas Unterthiner, Sjoerd Van Steenkiste, Karol Kurach, Raphael Marinier, Marcin Michalski, and Sylvain Gelly. Towards accurate generative models of video: A new metric & challenges. *arXiv preprint arXiv:1812.01717*, 2018.
- [36] Carl Vondrick, Hamed Pirsiavash, and Antonio Torralba. Generating videos with scene dynamics. *Advances in neural information processing systems*, 29, 2016.
- [37] Shihao Wang, Yingfei Liu, Tiancai Wang, Ying Li, and Xiangyu Zhang. Exploring object-centric temporal modeling for efficient multi-view 3d object detection. *arXiv preprint arXiv:2303.11926*, 2023.
- [38] Xiaofeng Wang, Zheng Zhu, Guan Huang, Xinze Chen, and Jiwen Lu. Drivedreamer: Towards real-world-driven world models for autonomous driving. *arXiv preprint arXiv:2309.09777*, 2023.
- [39] Yuqi Wang, Jiawei He, Lue Fan, Hongxin Li, Yuntao Chen, and Zhaoxiang Zhang. Driving into the future: Multiview visual forecasting and planning with world model for autonomous driving. *arXiv preprint arXiv:2311.17918*, 2023.
- [40] Yuqing Wen, Yucheng Zhao, Yingfei Liu, Fan Jia, Yanhui Wang, Chong Luo, Chi Zhang, Tiancai Wang, Xiaoyan Sun, and Xiangyu Zhang. Panacea: Panoramic and controllable video generation for autonomous driving. *arXiv preprint arXiv:2311.16813*, 2023.
- [41] Jay Zhangjie Wu, Yixiao Ge, Xintao Wang, Weixian Lei, Yuchao Gu, Wynne Hsu, Ying Shan, Xiaohu Qie, and Mike Zheng Shou. Tune-a-video: One-shot tuning of image diffusion models for text-to-video generation. *arXiv preprint arXiv:2212.11565*, 2022.
- [42] Kairui Yang, Enhui Ma, Jibin Peng, Qing Guo, Di Lin, and Kaicheng Yu. Bevcontrol: Accurately controlling street-view elements with multi-perspective consistency via bev sketch layout. *arXiv preprint arXiv:2308.01661*, 2023.
- [43] Zetong Yang, Li Chen, Yanan Sun, and Hongyang Li. Visual point cloud forecasting enables scalable autonomous driving. *arXiv preprint arXiv:2312.17655*, 2023.
- [44] Jiang-Tian Zhai, Ze Feng, Jinhao Du, Yongqiang Mao, Jiang-Jiang Liu, Zichang Tan, Yifu Zhang, Xiaoqing Ye, and Jingdong Wang. Rethinking the open-loop evaluation of end-to-end autonomous driving in nuscenes. *arXiv preprint arXiv:2305.10430*, 2023.
- [45] Beichen Zhang, Pan Zhang, Xiaoyi Dong, Yuhang Zang, and Jiaqi Wang. Long-clip: Unlocking the long-text capability of clip. *arXiv preprint arXiv:2403.15378*, 2024.
- [46] Lvmin Zhang and Maneesh Agrawala. Adding conditional control to text-to-image diffusion models. *arXiv preprint arXiv:2302.05543*, 2023.
- [47] Guosheng Zhao, Xiaofeng Wang, Zheng Zhu, Xinze Chen, Guan Huang, Xiaoyi Bao, and Xingang Wang. Drivedreamer-2: Llm-enhanced world models for diverse driving video generation. *arXiv preprint arXiv:2403.06845*, 2024.
- [48] Daquan Zhou, Weimin Wang, Hanshu Yan, Weiwei Lv, Yizhe Zhu, and Jiashi Feng. Magicvideo: Efficient video generation with latent diffusion models. *arXiv preprint arXiv:2211.11018*, 2022.

## A Method

### A.1 Detailed implementation of failure case driven framework

**Collecting Failure Cases.** Initially, we assess the performance of the base end-to-end model on the validation set. For this evaluation, we utilize the UniAD [13] base model as our starting point. We employ a metric, wherein a collision occurring within 3 seconds on the path planned by the algorithm qualifies a scenario as a failure case. Additionally, to gain further insights, we visualize both the perception results of the 3D boxes and the planning outcomes derived from the end-to-end model. Through this process, we identify and select failure cases for further analysis.

**Analyzing data pattern.** We initially anticipated that large visual-language models would be able to automatically pinpoint the reasons behind algorithm failures. However, our investigations revealed that a straightforward inquiry was insufficient for this purpose. Consequently, we devised a multi-round inquiry method leveraging VLM [1]. This approach enables a more precise analysis of the factors contributing to algorithm failures, as well as a detailed description of the key elements leading to such failures.

Specifically, we feed the visualization outcomes from the preceding step into VLM and prompt it to discern whether the primary cause of failure stems from perception or planning issues. In cases where perception is the culprit, the reasons can be further categorized into various factors such as nighttime darkness, challenges in recognizing large nearby objects, or the inability to identify rare object categories. On the other hand, if planning is identified as the source of failure, VLM can differentiate between scenarios like occlusion or infrequent interactions, including running a red light or crossing the road. Ultimately, based on the previously established reasons for failure, we prompt VLM to offer a precise account of the specific factors that led to the failure.

**Retrieving similar scenes.** Using the detailed image description, we employ BLIP-2 [19] to identify and retrieve scenes from the train set that closely correspond to the reasons behind the failure. This process involves quantifying the cosine similarity between embeddings extracted from both the image and the designated text input using BLIP-2. Based on this similarity measure, we then select and retrieve only the top- $k$  most relevant images.

**Updating Model.** Based on the identified potential failure scenarios, we created an extensive and varied image dataset utilizing *Delphi*. We obtained scene captions from VLM using corresponding sample tokens and employed these captions as input to generate analogous images with *Delphi*.

To augment data diversity, we employed a LLM to adjust the captions inputted into *Delphi*. This approach facilitated the alteration of scene descriptions to encompass various scene conditions and instance conditions, such as sunny, rainy, cloudy, Night, suburban, changing the color of the cars. Consequently, feeding these revised captions into *Delphi* resulted in the generation of a broader range of images.

However, we discovered that directly utilizing the generated failure scenes for training could result in overfitting. While the trained model excelled in the selected failure instances, its performance suffered in previously successful cases. Therefore, to mitigate this issue, we integrated our generated data with the complete train set for each fine-tuning session. This strategy proved effective in optimizing the model’s overall performance.

Ultimately, we trained the end-to-end model using this combined dataset, yielding a refined model that marked the commencement of the subsequent iteration of the improvement cycle.

## B Experiments

### B.1 Metrics

**Metrics about Quality and Controllability of Generated Video.** We evaluate the quality of the generated videos from two aspects: quality and controllability. Specifically, for quality, we use Frchet Inception Distance (FID) [7] to assess the realism of single-frame single-view images in the generated videos, Frchet Video Distance (FVD) [35] to evaluate the temporal consistency of

single-view videos, and CLIP scores (CLIP) [42] to assess the spatial consistency of single-frame multi-view images. For controllability, we utilize the popular BEV detection model StreamPETR [37] and end-to-end model [13] to evaluate the generated data and report the NDS score and the Average Collision Rate(Avg. Col. Rate) respectively, which comprehensively reflects the geometric alignment between the generated images and the BEV layout annotations. By using these evaluation metrics, we can ensure that the generated results maintain high standards in both quality and controllability.

**Metrics about Effectiveness of the Generated Video for End-to-End Model.** To evaluate the effectiveness of our proposed failure-case driven framework based upon the Delphi for the end-to-end model, we utilize the generated diverse training data to augment the end-to-end model’s origin training data. Specifically, we evaluate the performance of the end-to-end model by applying data augmentation on the nuScenes validation set and report the average collision rate.

## B.2 More Experimental Details

**Experimental Setting of the end-to-end model.** During the training phase, we utilize the model available on the UniAD official repository as our foundation for fine-tuning. To enhance the training process, we have decreased the learning rate by a factor of 10, setting it to  $2e-5$ . Additionally, we maintain consistency with the hyperparameters recommended on the UniAD repository, including the optimizer settings.

**Computation Efficiency and Hardware Requirements** We report the model complexity of our two model variants in Table 6. We will further provide the generated data on the nuScenes training set for the convenience of data augmentation.

Table 6: Model efficiency and hardware requirements.

| Model                   | Parameter | Inference Memeory&GPU | Inference Time | Train config     |
|-------------------------|-----------|-----------------------|----------------|------------------|
| multi-view single-frame | 0.5B      | 22GB(RTX3090)         | 4s / example   | 8×A100, 24 hours |
| multi-view multi-frame  | 1.1B      | 39GB(A100 40G)        | 4s / example   | 8×A800, 72 hours |

## B.3 Validating each components of our failure-case driven framework

As in Table 2, we compare in three aspects, data sampling strategy, number of generating cases and data engine validation.

**Data Sampling Strategy.** We evaluated different data sampling strategies, such as random sampling and failure-case targeted sampling. In the upper part of Table 2, we randomly selected various proportions of data samples from the training dataset and used the corresponding BEV layout and original scene captions to generate new data. In the lower part of Table 2, we retrieved training data with similar patterns to failure cases from the validation set and generated diverse weather data using the powerful control capabilities of the generative model. The newly generated data was mixed with the original data to train the end-to-end model. It was observed that the end-to-end model, enhanced through failure-case guided data augmentation, achieved the best performance. This demonstrates that the end-to-end model is under-trained in these failure cases, and feeding it more failure-case related training data can achieve optimal generalization performance with fewer computational resources.

**Numbers of Cases.** We investigated the quantity of data samples. We randomly sampled 14,065 and 28,130 training samples (approximately 50% and 100% of the entire training set) from the training set. The results generated by the configuration of the generative model on these samples were used for data augmentation. As shown in the upper part of Table 2, the performance of the end-to-end model worsened as the number of samples increased. This indicates that using training data with a style similar to the original training set can only help the model to a limited extent. Thus, it prompted us to consider increasing the diversity of the training data.

**Data Engine.** We tested various data generation engines, including Delphi and other state-of-the-art generative models Panacea [40], to compare their effectiveness in generating high-quality training data for model enhancement. From the three sets of comparison experiments, it can be seen that the

data generated by Delphi effectively improves the performance of the end-to-end model compared to other generative models. This is due to Delphi's superior fine control capabilities in scene generation, leading to more diverse training data for model tuning.